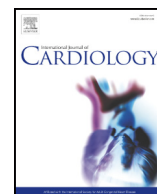




Contents lists available at ScienceDirect

International Journal of Cardiology

journal homepage: www.elsevier.com/locate/ijcard

The role of personalized atrial modeling in understanding atrial fibrillation mechanisms and improving treatment

Konstantinos N. Aronis^{a,b,1}, Rheeda Ali^{a,1}, Natalia A. Trayanova^{a,*}

^a Department of Biomedical Engineering and the Institute for Computational Medicine, Johns Hopkins University, Baltimore, MD, USA

^b Division of Cardiology, Johns Hopkins Hospital, Baltimore, MD, USA

ARTICLE INFO

Article history:

Received 28 December 2018

Received in revised form 24 January 2019

Accepted 28 January 2019

Available online xxxxx

ABSTRACT

Atrial fibrillation is the most common arrhythmia in humans and is associated with high morbidity, mortality and health-related expenses. Computational approaches have been increasingly utilized in atrial electrophysiology. In this review we summarize the recent advancements in atrial fibrillation modeling at the organ scale. Multi-scale atrial models now incorporate high level detail of atrial anatomy, tissue ultrastructure and fibrosis distribution. We provide the state-of-the art methodologies in developing personalized atrial fibrillation models with realistic geometry and tissue properties. We then focus on the use of multi-scale atrial models to gain mechanistic insights in AF. Simulations using atrial models have provided important insight in the mechanisms underlying AF, showing the importance of the atrial fibrotic substrate and altered atrial electrophysiology in initiation and maintenance of AF. Last, we summarize the translational evidence that supports incorporation of computational modeling in clinical practice for development of personalized treatment strategies for patients with AF. In early-stages clinical studies, AF models successfully identify patients where pulmonary vein isolation alone is not adequate for treatment of AF and suggest novel targets for ablation. We conclude with a summary of the future developments envisioned for the field of atrial computational electrophysiology.

© 2019 Elsevier B.V. All rights reserved.

1. Introduction

Computational approaches have been increasingly utilized over the recent years in atrial cardiac electrophysiology and specifically in the study of atrial fibrillation (AF). AF is the most common cardiac arrhythmia in the US¹ and world-wide [2], with an increasing prevalence, and significant morbidity, mortality and healthcare-related expenses associated with it [1,3,4]. Despite the progress in mapping technologies and catheter design, the current therapeutic approaches to AF have modest efficacy, particularly in patients with persistent AF, with recurrence rates up to ~50% [5–8]. The modest efficiency reflects, at least partially, the underlying complexity of the dynamic electroanatomical substrate [9] and our incomplete understanding of the mechanisms involved in the pathophysiology of the disease. Computational modeling and

simulations provide a framework of integrating multi-scale phenomena underlying AF and translating micro-scale experimental findings to whole-organ emergent behaviors (Fig. 1). Alongside with experimental electrophysiological investigations, computational modeling and simulations have a pivotal role in understanding the mechanisms underlying AF and designing novel, individualized therapeutic approaches. With recent technological advancements in high-performance distributed computing, atrial computational models are currently in early stages of clinical translation, beginning to contribute to patient-specific optimization of AF care.

In this review we focus on recent advancements in organ-scale atrial modeling and its applications in understanding AF mechanisms and developing personalized treatment approaches. We summarize studies that have taken place since our last review on the subject in 2014 [10]. We do not focus on ionic mechanism in AF as they are reviewed in an accompanying review [11]. For this, “personalization” refers to the use of patient-specific atrial geometry and fibrosis distribution to obtain patient-specific simulation results. Specifically, here we provide an overview of methods for developing 3D atrial models, including those with image-based realistic geometry. We then focus on the use of multi-scale atrial models to gain mechanistic insights in AF, and on the development of personalized treatment strategies for patients with AF. We conclude the review with a summary of the future developments envisioned for the field of 3D atrial computational electrophysiology.

Abbreviations: 1D, one-dimensional; 2D, two-dimensional; 3D, three-dimensional; AF, atrial fibrillation; APD, action potential duration; CT, computed tomography; ECGI, electrocardiographic imaging; LGE-MRI, late gadolinium enhanced magnetic resonance imaging; LA, left atrium; MRI, magnetic resonance imaging; RA, right atrium.

* Corresponding author at: Department of Biomedical Engineering and Institute for Computational Medicine, Johns Hopkins University, Hackerman 216, 3400 N. Charles Street, Baltimore, MD 21218, USA.

E-mail address: ntrayanova@jhu.edu (N.A. Trayanova).

¹ These authors have contributed equally to this work.

<https://doi.org/10.1016/j.ijcard.2019.01.096>

0167-5273/© 2019 Elsevier B.V. All rights reserved.

Please cite this article as: K.N. Aronis, R. Ali and N.A. Trayanova, The role of personalized atrial modeling in understanding atrial fibrillation mechanisms and improvi..., International Journal of Cardiology, <https://doi.org/10.1016/j.ijcard.2019.01.096>

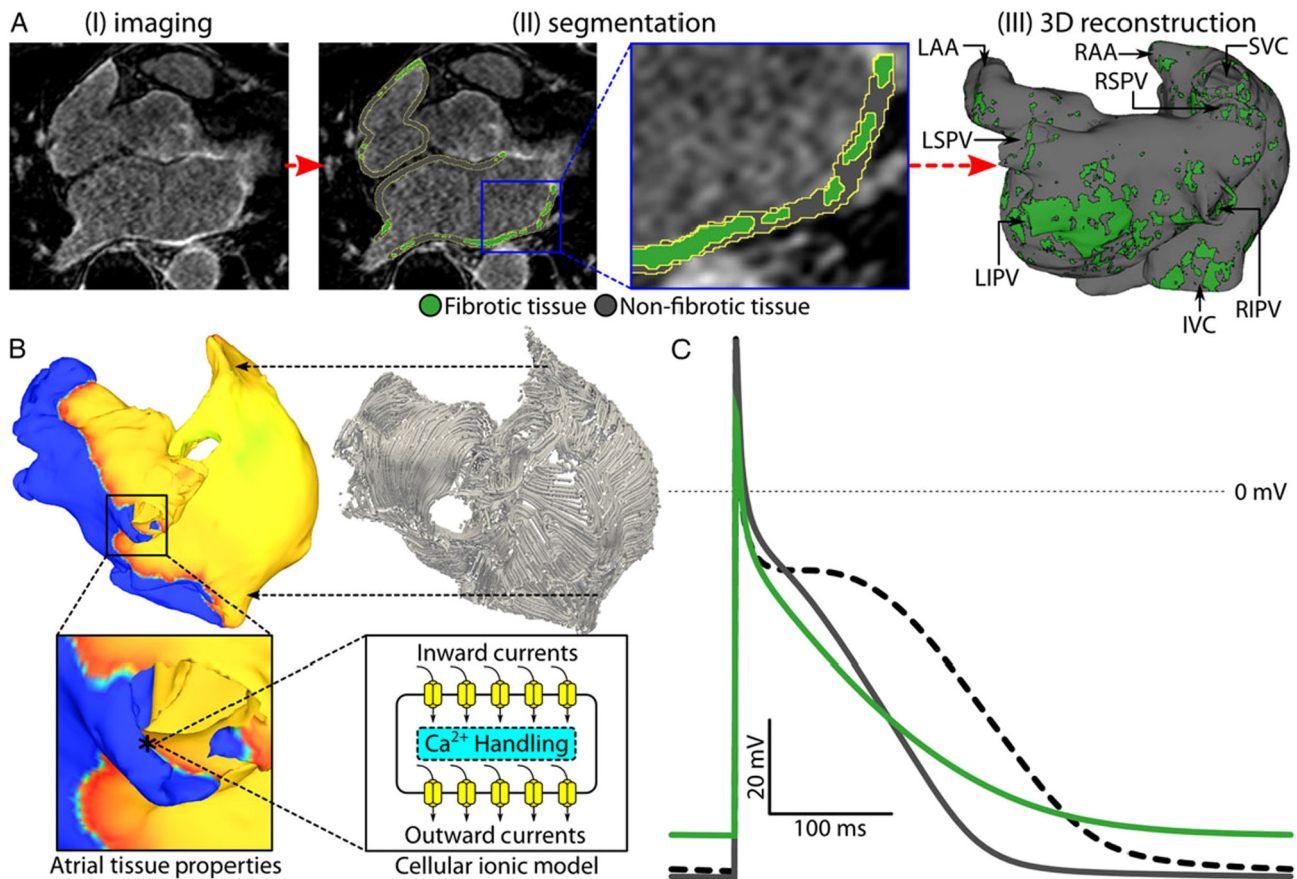


Fig. 1. Multi-scale model generation. Atrial models are constructed in 3 different spatial scales: organ-level scale, tissue-level scale, and cell-level scale. (A) Pipeline used to construct image-based organ-level scale models of the fibrotic human atria: (i) Representative LGE-MRI slice of the human atria; (ii) Segmentation of atrial tissue into fibrotic (green) and non-fibrotic (grey) regions; (iii) 3D reconstruction of atrial geometry with anatomical features labelled (RIPV/RSPV/LIPV/LSPV, right/left inferior/superior pulmonary veins; LAA, left atrial appendage; IVC/SVC, inferior/superior vena cava). Phenomena at this scale evolve over the micro-second to seconds temporal scale. (B) Electrical coupling of atrial cells at the tissue-level scale mediates propagation of bioelectric impulses, which originate at membrane level (action potentials in the cellular ionic model). Atrial fiber orientations, shown in the top right image, govern the preferential direction of electrical propagation. (C) Cell-level atrial electrophysiology: atrial action potentials obtained at a basic cycle length of 500 ms in fibrotic (green), non-fibrotic tissue (grey), and healthy tissue (dashed). Phenomena at this scale evolve at the microsecond temporal scale. (For interpretation of the references to colour in this figure legend, the reader is referred to the web version of this article.) Reproduced from [38].

2. Advancements in AF computational model development

2.1. Atrial geometrical models

Contemporary organ-level studies are performed on models with realistic atrial geometry. Models with realistic atrial geometry can be (a) 3D surface models (manifold), (b) full-thickness volumetric 3D models, and (c) 3D bilayer model.

Surface models represent atrial geometry as a 3D surface and neglect atrial wall thickness. 3D surface models have been reconstructed from computed tomography (CT) scans [12] or invasively-acquired electroanatomic maps [13–16]. Since the atria are thin-wall structures, 3D surface models accurately capture atrial geometry.

Full-thickness, volumetric 3D models have been reconstructed mostly from magnetic resonance imaging (MRI) [17–26], but also from CT scans [27,28]. Volumetric 3D models can accurately represent the transmural complexities and fine details of atrial anatomy, but have a significantly higher computational cost [10,29].

The bilayer model is an intermediate modeling approach, between 3D surface models and volumetric 3D models, where the atria are represented as two surfaces: an endocardial and an epicardial [30]. The bilayer model has been reconstructed from MRI [31–34] and CT scans [30,35]. This model is able to capture transmural heterogeneities as

they incorporate 2 surfaces, 2 fiber directions, major muscle bundles and discrete atrial coupling (Fig. 2A).

2.1.1. Detection and modeling of fibrosis

A critical development in organ-level atrial modeling is the inclusion of fibrotic structural remodeling associated with persistent AF. Atrial Fibrosis can be detected on late gadolinium enhancement magnetic resonance imaging (LGE-MRI) as areas of increased gadolinium uptake. Several thresholding techniques are used to differentiate between normal and fibrotic atrial myocardium [36].

Areas of fibrosis can be modeled by (a) changes in electrophysiological parameters resulting in alternations of tissue-scale propagation [10,37,38] and (b) stochastic removal of model elements in fibrotic areas resulting in percolation-like excitation dynamics [39]. Changes in electrophysiological parameters capture experimentally observed structural and ionic alternations present in fibrotic atrial tissue. Specifically: (a) down-regulation, hypo-phosphorylation and lateralization of connexin-43 is represented as a change in the tissue-scale conductivity and anisotropy ratio; (b) patchy collagen deposition is represented by introducing patchy areas of electrical isolation, and (c) fibroblast-induced remodeling is represented by introducing fibroblasts in the model, that affect the electrophysiological properties of neighboring cells *via* electrical coupling or paracrine mechanisms [10,37,38]. In the only study available to date assessing the validity of different fibrosis

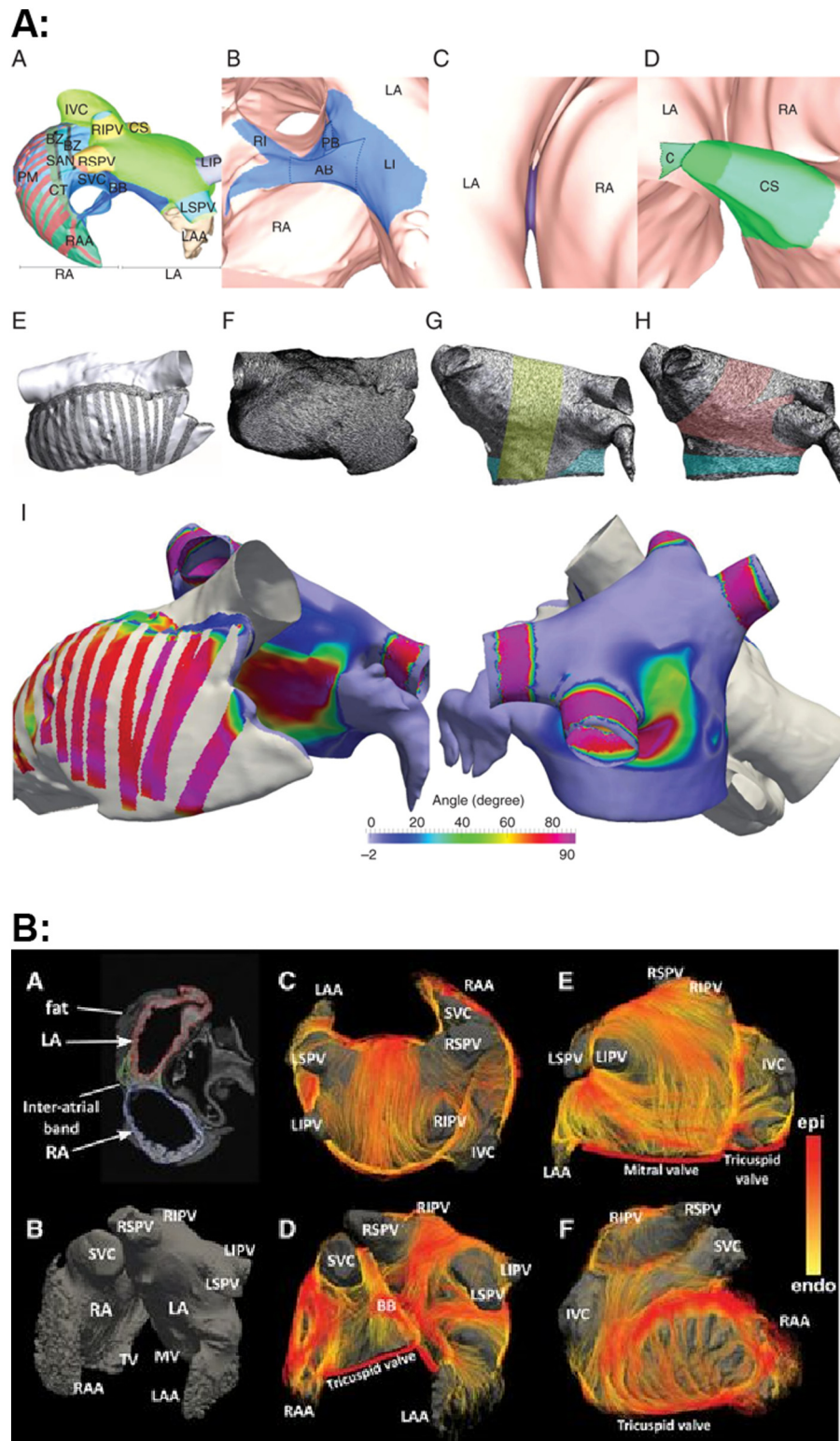


Fig. 2. A: Geometrical characteristics of the bilayer model. First row: General view (A) and transseptal connections (B–D). Bachmann’s bundle (blue), FO (purple), and CS (green) models are displayed. LA, RA, left and right atria; LI, RI, left and right insertions of the BB; AB, PB, anterior and posterior branches of the BB; C, connections between the CS and the LA. Second row: Fiber architecture. Right superior view of the *endo*- (E) and epicardial (F) layers of the RA. Anterior view of the *endo*- (G) and epicardial (H) layers of the LA including the septatrial (green) and septopulmonary (pink) bundles and the vestibule (blue). Third row: Angle map: difference of endocardial and epicardial fiber direction, in degrees (I). Grey (no value): only one layer is defined. The main differences are localized in the CT and the PM for the RA, and in the anterior and posterior walls and in PV for the LA [30]. **B:** Acquired geometry and fiber visualization results in human atria specimens. Left, Atrial geometry. A, Short-axis view of a nondiffusion-weighted image (b0) with superimposed segmentation of left atrium (LA; red), right atrium (RA; blue), and interatrial bundles (green). Fat tissue surrounding the atria is excluded from the segmentation. B, Anterior view of left and right atria created from T1-weighted images; the dark grey volume represents lumen. Right, Fiber visualization using tractography. C, Posterior view of atrial roof. D, Anterior view. E, Inferior and left lateral views. F, View of right atrium. Colour encodes the local distance to the endocardial shell: yellow is the endocardial layer, and red is the epicardial layer. BB indicates Bachman bundle; IVC, inferior vena cava; LAA, left atrial appendage; LIPV, left inferior pulmonary vein; LSPV, left superior pulmonary vein; MV, mitral valve; RAA, right atrial appendage; RIPV, right inferior pulmonary vein; RSPV, right superior pulmonary vein; SVC, superior vena cava; and TV, tricuspid valve. (For interpretation of the references to colour in this figure legend, the reader is referred to the web version of this article.) Modified with permission from [42].

modeling approaches, the number of phase singularities seen with percolation was closer to the clinical values [32]. However, this study included patient-specific models from only 3 patients and larger studies are needed.

2.1.2. Atrial fiber orientation

Incorporating fiber orientation in organ-scale 3D models is important for accurate simulations [40]. Existing atrial models incorporate fiber orientation determined using semi-automatic tools and fiber orientation atlases derived from histology [38]. Fastl et al. used a sophisticated Laplace-based algorithm to assign fiber orientation to models reconstructed from cardiac computed tomography images with variable wall thickness and complex atrial architecture [27]. The estimated left atrial (LA) myofiber orientation matched previously reported calculated LA myofiber orientations [21,41]. In simulations, the local activation times were consistent with described values in the literature [27]. The methodology by Fastl et al. establishes a pipeline that provides a robust framework for the rapid development of personalized models accounting for detailed anatomy and microstructure.

Diffusion tensor MRI sequence has been used to capture the micro-architecture of myofibers in the human atria *ex-vivo*, including the major distinct atrial bundles ($n = 8$) [42]. There are currently no available imaging modalities that can visualize fiber orientation in humans *in vivo*. For this, *ex-vivo* diffusion tensor MRI images have been used in the development of maps of fiber organization that are more accurate than the currently available histology-derived atlases (Fig. 2B). This fiber architecture can be incorporated into atrial models *via* co-registration and other morphing methodologies [43,44]. In an *ex vivo* study of swine atrial preparations, atrial anatomy and fiber orientation were directly and simultaneously reconstructed from optical coherence tomography imaging. Simulations using organ-specific fiber orientation accurately predicted activation time maps derived by optical mapping experiments [45]. The feasibility of optical coherence tomographic imaging as a method to generate atrial models has not been examined to date in humans.

Improvement of patient-specific atrial fiber representation in models can be achieved with (a) development of more accurate atlases of fiber orientation, (b) development of image-based fiber atlases that are representative of a wide range of atrial sizes and shapes (c) improvement of registration and morphing techniques used to transform fiber orientation from one anatomy to another, and ultimately (d) development of new imaging methodologies that could allow for *in-vivo* visualization of myofibers.

3. Mechanistic insights in AF using computational modeling

Atrial computational modeling has been used to provide insights in the fundamental mechanisms involved in initiation and perpetuation of AF. Increased pulmonary vein ectopy is the primary mechanism of arrhythmia initiation in paroxysmal AF [46]. There are limited modeling studies evaluating pulmonary vein ectopy, that have been previously reviewed [10]. Recently, Roney et al. demonstrated that the electrophysiological properties and the extent of fibrosis of the pulmonary vein are associated with patient-specific susceptibility to AF initiation and maintenance [31].

Recent clinical and experimental studies provide evidence that re-entrant drivers within regions of structural inhomogeneities have a significant role in maintenance of persistent AF [47]. However, the exact mechanisms of initiation and maintenance of these drivers remain incompletely understood. Key features of the AF-induced electroanatomical remodeling that have a significant role in re-entrant driver dynamics, as reviewed below, are (a) atrial fibrosis and fibrosis distribution, (b) atrial wall thickness, and (c) development of APD alternans. Although autonomic innervation of the atria has a significant role in AF [48], the distribution and remodeling of autonomic nerve fibers are not currently incorporated in atrial models, primarily due to

inability to visualize these structures with clinically available imaging technologies.

3.1. Role of fibrosis in AF dynamics

Patient-specific distribution of fibrosis is a significant determinant of initiation and maintenance of AF, as well as localization of AF re-entrant drivers. In a sensitivity study using realistic atrial geometry, the degree and distribution of fibrosis and the choice of fibrosis implementation technique had a larger effect on re-entrant driver localization compared to variations in tissue wavelength [34]. In a different sensitivity analysis using patient-specific atrial models, localization of re-entrant driver trajectories was determined by scar distribution while changes in APD or conduction velocity enhanced or attenuated the likelihood that a re-entrant driver anchored to a specific site [17].

Although the presence of diffuse atrial fibrosis is sufficient for induction of AF in simulations [49], patient-specific distribution of fibrosis largely affects simulated AF dynamics [20,38,39,50]. Advances in clinical imaging modalities have rendered them capable of resolving the unique fibrosis spatial patterns present in the atria of each individual patient [37]. Patient-specific 3D atrial models, with atrial geometry and fibrosis distribution derived from clinically available LGE-MRI demonstrate that AF drivers persist only in areas with highly specific fibrotic spatial patterns ($N = 22$) [38]. Fibrotic spatial patterns were characterized by calculating maps of fibrosis density and fibrosis entropy. Local fibrosis density indicates the proportion of fibrotic elements among all elements surrounding the given location, while local fibrotic entropy quantifies the degree of disorganization between fibrotic and non-fibrotic elements in the local neighborhood. Re-entrant drivers persisted in fibrotic boundaries zone characterized by high fibrotic density and fibrotic entropy (Fig. 3) [38]. Fibrotic patterns with high density and entropy correspond to atrial areas with a high degree of intermingling between fibrotic and non-fibrotic tissue. Similar results have been obtained in a smaller study that utilized a different fibrosis modeling approach, where fibrosis was represented as myocyte-fibroblast coupling dependent on the LGE-MRI intensity ($N = 3$). Re-entrant drivers stabilized in the border zones of patchy fibrosis in all 3 patient-specific atrial models [50]. A biphasic behavior in re-entrant driver development in response to fibrosis density has been described in 3D atrial models where fibrosis is modeled as percolation-like excitation dynamics [39].

Experimental validation of the association between patient-specific fibrosis distribution and re-entrant driver localization in AF has been provided from a study in an *ex vivo* atrial preparation from a patient with chronic AF [21]. The atrial model reconstructed from LGE-MRI and histology data demonstrated that AF re-entrant drivers coalesce in atrial areas of distinct structural “fingerprints,” which consist of a combination of intermediate wall thickness, intermediate fibrosis, and twisted myofiber orientation. Re-entrant driver localization predicted by simulations was confirmed with direct visualization using optical mapping. Removal of fibrosis from simulations rendered the atrial model non-inducible for AF [21].

3.2. Wall thickness heterogeneity and its implications for AF

Atrial wall thickness heterogeneity is a structural property of the atria that has been recently associated with re-entrant driver dynamics during AF [15,19]. In idealized and realistic simulations of atrial models, re-entrant drivers drift from thicker to thinner regions along ridge-line structures, indicating that atrial wall thickness is critical in determining the re-entrant driver trajectory [15,19]. In 3D bi-atrial models reconstructed from MRIs of healthy volunteers ($N = 4$) and patients with AF ($N = 2$) atrial wall thickness was an important determinant for re-entrant driver trajectory in the right atrium (RA), while in the LA, re-entrant driver trajectory was primarily influenced by fibrosis distribution [19].

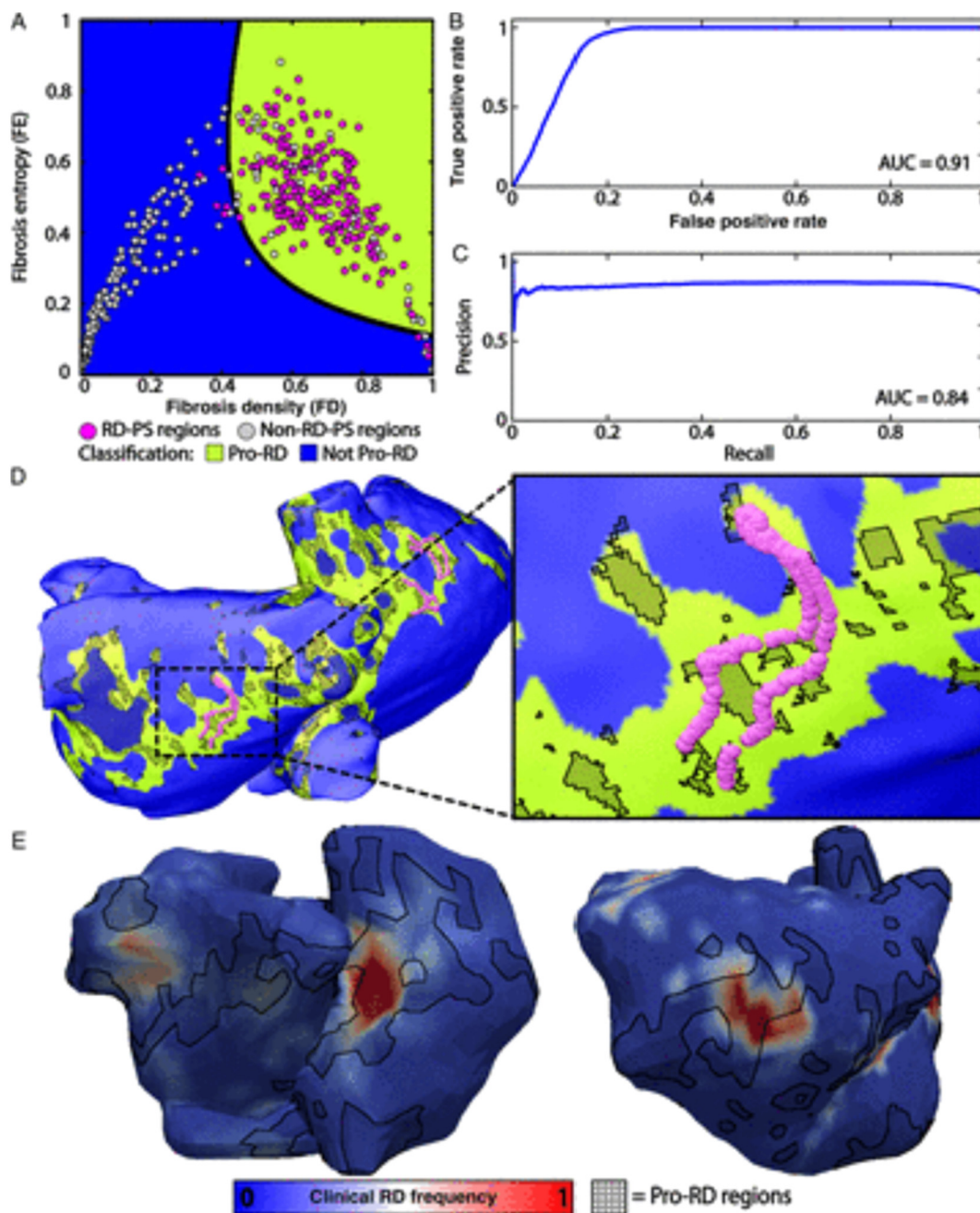


Fig. 3. Machine learning classification of RD-PS and non-RD-PS regions based on FD and FE. (A) Classification of RD-PS and non-RD-PS regions. The polynomial equation that separated RD-PS (purple circles) and non-RD-PS regions (yellow circles) is indicated with a black line. The FD and FE values that characterized RD-PS regions and non-RD-PS regions are indicated in green (Pro-RD) and blue (Not Pro-RD), respectively. (B) Receiver operating characteristic analysis of the machine learning algorithm. The AUC for this plot was 0.91. (C) Precision-recall analysis of the machine learning algorithm. The AUC for this plot was 0.84. Together, (B) and (C) indicate robust classification. (D) Location of RD-PSs in example patient overlaid on the regions of the atria with the characteristic FD and FE values predicted to contain RD-PSs (green). (E) Comparison with clinical results. Example atrial ECGI maps are shown for two patient models. Red colour indicates regions of greatest frequency of RD-PSs occurrence. (For interpretation of the references to colour in this figure legend, the reader is referred to the web version of this article.)

Modified with permission from [38].

3.3. APD alternans and AF dynamics

Atrial repolarization alternans, defined as the beat-to-beat alternation in APD, have been associated with increased propensity for initiation of AF in animal models [51,52] and limited human data [53]. Computational modeling has provided useful insight in the ionic mechanisms underlying atrial repolarization alternans as well as the mechanisms linking the cellular phenomenon of repolarization alternans to the emergent macroscopic behavior of AF in humans [54,55]. The

potential ionic mechanisms of atrial repolarization alternans were explored in a sensitivity analysis [54] of simulations that used a biophysically-detailed atrial model and realistic 3D atrial geometry. That study found that decreased ryanodine receptor inactivation resulted in augmentation of Ca^{2+} alternans and was the only electrophysiologic alteration that resulted in repolarization alternans, as seen clinically at slower heart rates. These results suggest that ryanodine receptor kinetics play a critical role in altered Ca^{2+} homeostasis, driving proarrhythmic repolarization alternans in patients with AF [54]. In

organ-scale simulations, elevated Ca^{2+} alternans propensity due to decreased ryanodine receptor inactivation, and development of repolarization alternans at slower heart rates, resulted in increased ectopy-induced arrhythmia vulnerability, complexity, and persistence due to increased repolarization heterogeneity and wavebreak [55].

4. Therapeutic applications of computational modeling

4.1. AF Ablation strategy

The most revolutionizing translational application of atrial modeling is the potential for development of personalized AF ablation strategies, specifically tailored to each patient's unique electroanatomical atrial substrate. Here we summarize early stage clinical studies supporting the feasibility of patient-specific, model-derived AF ablation strategies.

4.1.1. Re-entrant drivers as ablation targets

McDowell et al. was the first to demonstrate in a proof-of-concept study that patient-specific simulations of atrial models reconstructed from LGE-MRI ($N = 4$) can detect AF ablation targets. The virtual ablation strategy used in this study, delivered ablation lesions in atrial regions encompassing the meander of persistent re-entrant drivers rendering the atrial model non-inducible for AF [20]. In subsequent studies, patient-specific simulations have revealed areas harboring re-entrant drivers that cannot be identified with currently available clinical methods (known as "latent re-entrant drivers") [23,24]. The currently available methods for localization of re-entrant driver trajectories during AF, in the clinical setting, are focal impulse and rotor mapping (FIRM) [56,57], and electrocardiographic imaging (ECGI) [58]. AF patients that underwent FIRM-guided ($N = 11$) [23] and ECGI-guided ($N = 12$) [24] re-entrant driver ablation, in addition to PVI, had a significantly higher risk for AF recurrence, if the re-entrant driver locations that were ablated where different from those identified in simulations. These results suggest that a therapeutic approach that combines clinical visualization of re-entrant drivers with simulations identifying "latent re-entrant drivers" can improve AF ablation outcomes.

The exact locations where re-entrant drivers are observed during AF simulations, and thus the ablation targets, are significantly affected by the electrophysiological properties of the model used. In a sensitivity analysis, 10% variation of atrial APD or conduction velocity resulted in different likelihood that a re-entrant driver would anchor at a specific location [17]. Considering the inability of current models to capture patient-specific, region-specific and situation-specific alternations in cardiac electrophysiology, there is some uncertainty in the exact locations where re-entrant drivers are predicted to occur by simulations. Hakim et al. [59] demonstrated that this uncertainty can be substantially mitigated by conducting virtual re-entrant driver ablations followed by repeat simulations to evaluate for, and ablate any emergent re-entrant drivers. Specifically, simulations were performed in patient-specific atrial models ($N = 12$) using "average human AF" electrophysiology and $\pm 10\%$ variation in APD or conduction velocity. Re-entrant drivers induced under the average electrophysiology condition were virtually ablated and the AF induction protocol was re-applied. Twenty-one emergent re-entrant drivers were observed in 9/12 atrial models. Most emergent re-entrant drivers (71%) were at close proximity (<0.1 cm) to sites where re-entrant drivers were seen pre-ablation in simulations using $\pm 10\%$ variation in APD or conduction velocity.

Atrial modeling constitutes a unique tool for designing ablation strategies that minimize ablation-induced atrial pro-arrhythmia. Atrial macro-reentrant tachycardias or left-atrial flutters frequently occur after AF ablation due to modifications of the electrophysiological substrate introduced by the ablation lesions [60,61]. Patient-specific atrial modeling was applied in a study of patients who were successfully treated for AF via catheter ablation, but experienced recurrent post-procedure left atrial flutter ($N = 10$) [26]. A virtual electrophysiological study was able to induce left atrial flutter in most atrial models (7/10). A

novel algorithm that abstracts the simulated re-entrant propagation using principles of graph theory was used to predict optimal ablation lesions that render arrhythmia initiation impossible with the minimal lesion burden. This algorithm is known as the "minimal cut algorithm" i.e. the minimum number of edges removed from a graph that separate the left atrium in two disconnected components. Ablation lesions predicted by the minimal cut algorithm rendered 4/7 models non-inducible for left atrial flutter after the first application of the algorithm and 7/7 models non-inducible after a second application.

4.1.2. Ablation strategies other than re-entrant drivers targeting

AF ablation strategies other than re-entrant driver targeting have been used in the clinical setting. Typically, these strategies are adjuvant to pulmonary vein isolation and include empirical lines in the left atrium, entire posterior wall electrical isolation, and ablation of complex fractionated atrial electrograms, but have limited clinical efficiency [8]. Surgical Maze procedures [62] or hybrid approaches [63] are alternative rhythm control strategies, particularly suitable for patients with persistent AF, but are more invasive than catheter-based ablation. Atrial models have been used to optimize different surgical Maze procedures, and this has been previously reviewed [10].

Atrial models reconstructed from cardiac computed tomography images of patients with AF ($N = 20$) have been used to compare the efficiency of five adjuvant ablation strategies *in silico*. These strategies included a combination of circumferential pulmonary vein isolation, lines and complex fractionated atrial electrogram ablation; circumferential pulmonary vein isolation with a posterior box isolation and anterior line ablation was the most efficient ablation strategy [28]. The efficacy of these five adjuvant ablation strategies was subsequently evaluated in a prospective clinical trial, of 108 patients with persistent AF that were randomized to receive either empirical ablation or ablation guided by patient-specific modeling. The study demonstrated that modeling-guided selection of the adjuvant lesion geometry is safe and non-inferior to empirical AF ablation [12]. The atrial models used in these studies were homogeneous atria models and did not incorporate patient-specific fibrosis.

The efficacies of three different ablation strategies were compared in a simulation study that used the bilayer atrial modeling approach and included patient-specific fibrosis derived from LGE-MRI [35]. The ablation strategies that were evaluated were (i) pulmonary vein isolation, roof, and mitral lines; (ii) circles, perforated circles, lines, and crosses delivered near re-entrant driver locations identified by phase mapping; and (iii) lines streamlining the sequence of electrical activation during sinus rhythm. The most effective strategy was to ablate in the streamline of the activation sequence during sinus rhythm (Fig. 4) [35]. Last, in a cellular automaton model representing AF as multiple meandering wavelets, the greatest reduction in multiple wavelet re-entry burden was observed with transection of the tissue into regions that could support equivalent wavelet populations [64]. These results suggest that computational modeling could be used to select patients that would benefit from ablation lesions adjuvant to pulmonary vein isolation, as well as to develop novel ablation strategies different from AF re-entrant drivers targeting.

4.2. Pharmacotherapy

Antiarrhythmic drug therapy constitutes a first-line treatment option for patients with AF [65]. However, rhythm control of AF with antiarrhythmic medications has only moderate efficacy. The role of atrial modeling in AF pharmacotherapy is multi-faceted. Atrial modeling is used to (a) screen for potential targets of antiarrhythmic medications [66], (b) predict the efficacy of medications under development [66] [67], (c) provide insights in the mechanisms through which antiarrhythmic medications terminate or fail to terminate AF [68], and (d) personalize antiarrhythmic strategy to patients with different electroanatomical substrate [69,70].

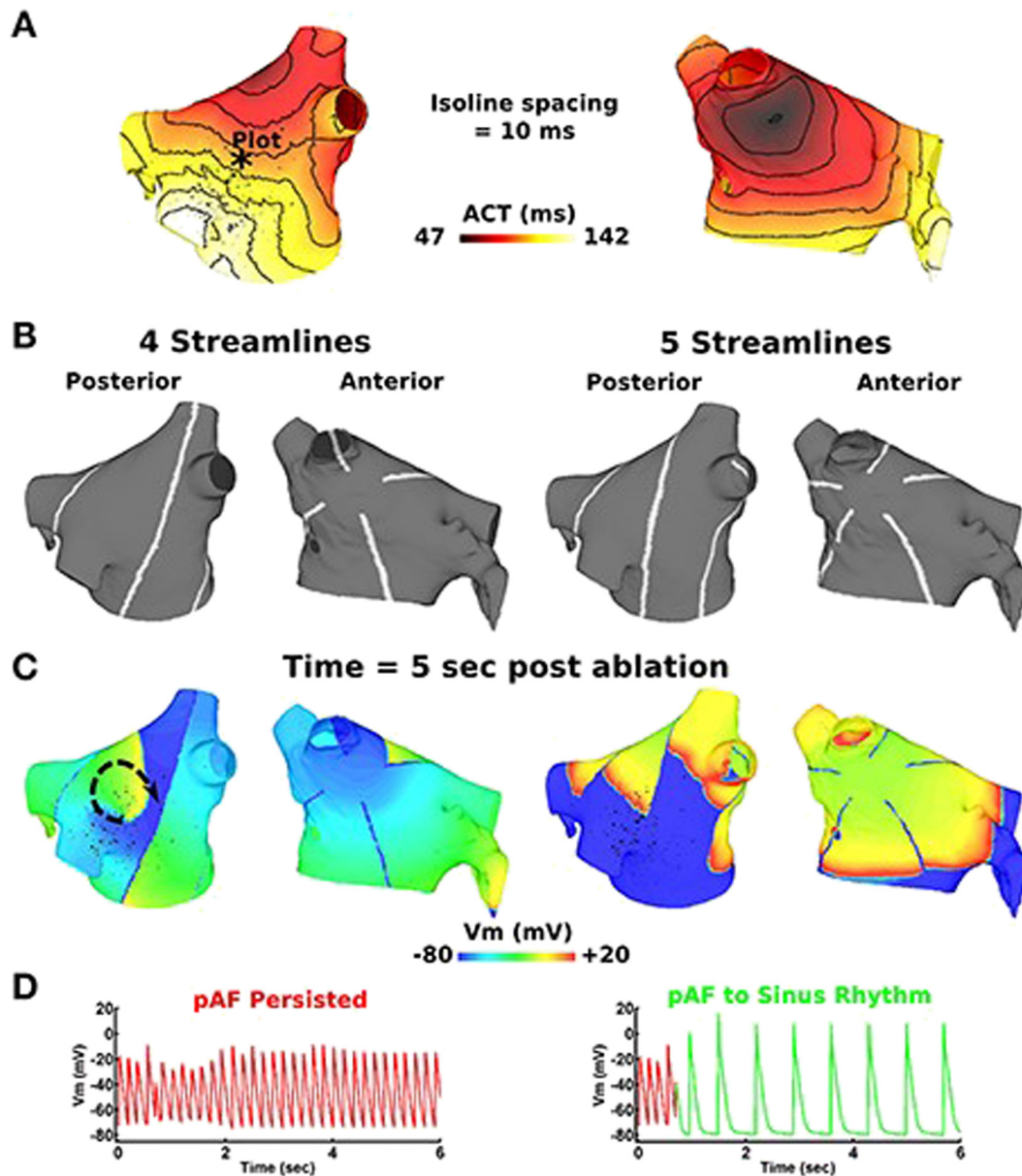


Fig. 4. Streamlining the sequence of LA activation during sinus rhythm with >4 lines effectively terminates pAF from RSPV pacing. (A) LA activation times during sinus rhythm at 86 beats per min. (B) four or five RFA lines that streamline the activation time sequence in (A). (C) Transmembrane voltage (V_m) maps 5 s post streamlining showing unsuccessful pAF termination with four RFA lines, but successful pAF termination with five RFA lines. (D) V_m plotted at the point indicated by the * in (A) before and after streamlining with four and five RFA lines. Modified with permission from [35].

5. Future perspectives

Current atrial modeling approaches have some limitations that need to be addressed in future studies [62]. First, different fibrosis representation methodologies should be validated in clinical studies. Second, there is a need for improved representation of patient-specific atrial fiber orientation. Third, future atrial models should incorporate autonomic innervation and remodeling as it has an important role in AF pathophysiology. Fourth, current atrial models are unable to capture the progression of the disease in terms of the patient-specific and region-specific electrophysiological remodeling of the non-fibrotic myocardium. Last, atrial models are computationally demanding, and this limits their scalability.

Atrial modeling necessitates continuous adaptation to integrate (a) new experimental findings regarding the pathophysiology of atrial fibrillation that would enable for more accurate mechanistic and clinical predictions, and (b) new computer science approaches that would improve execution time and scalability of these computationally-intensive

approaches. The advancement of atrial modeling is strongly dependent on developments in experimental methodologies and availability of clinical electrophysiological data, which are essential to constrain, enrich, and validate the models. Machine learning approaches have the potential to be combined with computational modeling to improve their predictive accuracy by both providing means to comprehensively analyze the wealth of high-dimensional complex spatiotemporal data produced by atrial models, and by incorporating a wide range of clinical data in the predictive algorithms [71]. Future research is needed in developing the methods necessary to enable computational modeling to be executed real-time. Real-time performance can be obtained by implementing models in computer hardware such as field-programmable gate arrays. There are ongoing efforts on this direction in ventricular tachycardia modeling, but still in very early stages of development [72].

Utilization of atrial modeling for mechanistic insights in AF will continue to grow in a virtuous cycle with basic cardiac electrophysiology experimental advances. Given the promising results in early-stage

clinical studies, the immediately next milestone for atrial modeling is to be tested in randomized clinical trials where the efficiency of simulation-derived ablation targets will be tested against standard of care. End-points in such randomized clinical trials should include improvement in sinus rhythm maintenance and complications rate, reduction in procedure time, minimization of area of atrial tissue ablated. The “personalized computational electrophysiology laboratory” is not only a reality, but lies at the lancet of AF research, and is on a trajectory to be adopted in clinical practice.

Conflict of interest

The authors report no relationships that could be construed as a conflict of interest.

Acknowledgements

Funding Sources: This work was supported by funding support from National Institutes of Health [DP1-HL123271, U01-HL141074 to NT]; National Institutes of Health award 5T32HL007227-42 to K.N.A. Leducq [16CVD02 to NT]; a fellowship from Johns Hopkins University to RA.

References

- [1] E.J. Benjamin, M.J. Blaha, S.E. Chiuve, M. Cushman, S.R. Das, R. Deo, S.D. de Ferranti, J. Floyd, M. Fornage, C. Gillespie, C.R. Isasi, M.C. Jimenez, L.C. Jordan, S.E. Judd, D. Lackland, J.H. Lichtman, L. Lisabeth, S. Liu, C.T. Longenecker, R.H. Mackey, K. Matsushita, D. Mozaffarian, M.E. Mussolino, K. Nasir, R.W. Neumar, L. Palaniappan, D.K. Pandey, R.R. Thiagarajan, M.J. Reeves, M. Ritchey, C.J. Rodriguez, G.A. Roth, W.D. Rosamond, C. Sasson, A. Towfighi, C.W. Tsao, M.B. Turner, S.S. Virani, J.H. Voeks, J.Z. Willey, J.T. Wilkins, J.H. Wu, H.M. Alger, S.S. Wong, P. Muntner, American heart association statistics C and stroke statistics S. Heart disease and stroke statistics-2017 update: a report from the American Heart Association, *Circulation* 135 (2017) e146–e603.
- [2] F. Rahman, G.F. Kwan, E.J. Benjamin, Global epidemiology of atrial fibrillation, *Nat. Rev. Cardiol.* 11 (2014) 639–654.
- [3] S.P. Johnsen, L.W. Dalby, T. Tackstrom, J. Olsen, A. Fraschke, Cost of illness of atrial fibrillation: a nationwide study of societal impact, *BMC Health Serv. Res.* 17 (2017) 714.
- [4] M.S. Vaughan Sarrazin, M. Jones, A. Mazur, P. Cram, P. Ayyagari, E. Chrischilles, Cost of hospital admissions in Medicare patients with atrial fibrillation taking warfarin, dabigatran, or rivaroxaban, *J. Am. Coll. Cardiol.* 69 (2017) 360–362.
- [5] J.L. Pallisgaard, G.H. Gislason, J. Hansen, A. Johannessen, C. Torp-Pedersen, P.V. Rasmussen, M.L. Hansen, Temporal trends in atrial fibrillation recurrence rates after ablation between 2005 and 2014: a nationwide Danish cohort study, *Eur. Heart J.* 39 (2018) 442–449.
- [6] S. Kircher, A. Arya, D. Altmann, S. Rolf, A. Bollmann, P. Sommer, N. Dagues, S. Richter, O.A. Breithardt, B. Dinov, D. Husser, C. Eitel, T. Gaspar, C. Piorkowski, G. Hindricks, Individually tailored vs. standardized substrate modification during radiofrequency catheter ablation for atrial fibrillation: a randomized study, *Europace* (2017) <https://doi.org/10.1093/europace/eux310> Epub ahead of print.
- [7] S. Conti, R. Weerasooriya, P. Novak, J. Champagne, H.E. Lim, L. Macle, Y. Khaykin, A. Pantano, A. Verma, Contact force sensing for ablation of persistent atrial fibrillation: a randomized, multicenter trial, *Heart Rhythm.* 15 (2018) 201–208.
- [8] A. Verma, C.Y. Jiang, T.R. Betts, J. Chen, I. Deisenhofer, R. Mantovan, L. Macle, C.A. Morillo, W. Haverkamp, P. Weerasooriya, J.P. Albenque, S. Nardi, E. Menardi, P. Novak, P. Sanders, S.A.I. Investigators, Approaches to catheter ablation for persistent atrial fibrillation, *N. Engl. J. Med.* 372 (2015) 1812–1822.
- [9] D.H. Lau, D. Linz, U. Schotten, R. Mahajan, P. Sanders, J.M. Kalman, Pathophysiology of paroxysmal and persistent atrial fibrillation: rotors, foci and fibrosis, *Heart Lung Circ.* 26 (2017) 887–893.
- [10] N.A. Trayanova, Mathematical approaches to understanding and imaging atrial fibrillation: significance for mechanisms and management, *Circ. Res.* 114 (2014) 1516–1531.
- [11] J. Heijman, E. Grandi, Computational modeling: what it tell us about AF mechanisms and therapy? *Int. J. Cardiol.* (2019).
- [12] J. Shim, M. Hwang, J.S. Song, B. Lim, T.H. Kim, B. Joung, S.H. Kim, Y.S. Oh, G.B. Nam, Y.K. On, S. Oh, Y.H. Kim, H.N. Pak, Virtual in-silico modeling guided catheter ablation predicts effective linear ablation lesion set for longstanding persistent atrial fibrillation: multicenter prospective randomized study, *Front. Physiol.* 8 (2017) 792.
- [13] C. Corrado, S. Williams, R. Karim, G. Plank, M. O'Neill, S. Niederer, A work flow to build and validate patient specific left atrium electrophysiology models from catheter measurements, *Med. Image Anal.* 47 (2018) 153–163.
- [14] M. Hwang, B. Lim, J.S. Song, H.T. Yu, A.J. Ryu, Y.S. Lee, B. Joung, E.B. Shim, H.N. Pak, Ganglionated plexi stimulation induces pulmonary vein triggers and promotes atrial arrhythmogenicity: in silico modeling study, *PLoS One* 12 (2017), e0172931.
- [15] S.R. Kharche, I.V. Biktasheva, G. Seemann, H. Zhang, V.N. Biktashev, A computer simulation study of anatomy induced drift of spiral waves in the human atrium, *Biomed. Res. Int.* 2015 (2015) 731386.
- [16] B. Lim, M. Hwang, J.S. Song, A.J. Ryu, B. Joung, E.B. Shim, H. Ryu, H.N. Pak, Effectiveness of atrial fibrillation rotor ablation is dependent on conduction velocity: an in-silico 3-dimensional modeling study, *PLoS One* 12 (2017), e0190398.
- [17] D. Deng, M.J. Murphy, J.B. Hakim, W.H. Franceschi, S. Zahid, F. Pashakhanloo, N.A. Trayanova, P.M. Boyle, Sensitivity of reentrant driver localization to electrophysiological parameter variability in image-based computational models of persistent atrial fibrillation sustained by a fibrotic substrate, *Chaos* 27 (2017), 093932.
- [18] M.W. Krueger, K.S. Rhode, M.D. O'Neill, C.A. Rinaldi, J. Gill, R. Razavi, G. Seemann, O. Doessel, Patient-specific modeling of atrial fibrosis increases the accuracy of sinus rhythm simulations and may explain maintenance of atrial fibrillation, *J. Electrocardiol.* 47 (2014) 324–328.
- [19] A. Roy, M. Varela, O. Aslanidi, Image-based computational evaluation of the effects of atrial wall thickness and fibrosis on re-entrant drivers for atrial fibrillation, *Front. Physiol.* 9 (2018) 1352.
- [20] K.S. McDowell, S. Zahid, F. Vadakkumpadan, J. Blauer, R.S. MacLeod, N.A. Trayanova, Virtual electrophysiological study of atrial fibrillation in fibrotic remodeling, *PLoS One* 10 (2015), e0117110.
- [21] J. Zhao, B.J. Hansen, Y. Wang, T.A. Csepe, L.V. Sul, A. Tang, Y. Yuan, N. Li, A. Bratasz, K.A. Powell, A. Kilic, P.J. Mohler, P.M.L. Janssen, R. Weiss, O.P. Simonetti, J.D. Hummel, V.V. Fedorov, Three-dimensional integrated functional, structural, and computational mapping to define the structural “fingerprints” of heart-specific atrial fibrillation drivers in human heart ex vivo, *J. Am. Heart Assoc.* 6 (2017).
- [22] M. Alessandrini, M. Valinoti, L. Unger, T. Oesterlein, O. Dossel, C. Corsi, A. Loewe, S. Severi, A computational framework to benchmark basket catheter guided ablation in atrial fibrillation, *Front. Physiol.* 9 (2018) 1251.
- [23] P.M. Boyle, J.B. Hakim, S. Zahid, W.H. Franceschi, M.J. Murphy, A. Prakosa, K.N. Aronis, T. Zghaib, M. Balouch, E.G. Ipek, J. Chrispin, R.D. Berger, H. Ashikaga, J.E. Marine, H. Calkins, S. Nazarian, D.D. Spragg, N.A. Trayanova, The fibrotic substrate in persistent atrial fibrillation patients: comparison between predictions from computational modeling and measurements from focal impulse and rotor mapping, *Front. Physiol.* 9 (2018) 1151.
- [24] P.M. Boyle, J.B. Hakim, S. Zahid, W.H. Franceschi, M.J. Murphy, E.J. Vigmond, R. Dubois, M. Haissaguerre, M. Hocini, P. Jais, N.A. Trayanova, H. Cochet, Comparing reentrant drivers predicted by image-based computational modeling and mapped by electrocardiographic imaging in persistent atrial fibrillation, *Front. Physiol.* 9 (2018) 414.
- [25] T.N. Phung, C.B. Moyer, P.T. Norton, J.D. Ferguson, J.W. Holmes, Effect of ablation pattern on mechanical function in the atrium, *Pacing Clin. Electrophysiol.* 40 (2017) 648–654.
- [26] S. Zahid, K.N. Whyte, E.L. Schwarz, R.C. Blake 3rd, P.M. Boyle, J. Chrispin, A. Prakosa, E.G. Ipek, F. Pashakhanloo, H.R. Halperin, H. Calkins, R.D. Berger, S. Nazarian, N.A. Trayanova, Feasibility of using patient-specific models and the “minimum cut” algorithm to predict optimal ablation targets for left atrial flutter, *Heart Rhythm.* 13 (2016) 1687–1698.
- [27] T.E. Fastl, C. Tobon-Gomez, A. Crozier, J. Whitaker, R. Rajani, K.P. McCarthy, D. Sanchez-Quintana, S.Y. Ho, M.D. O'Neill, G. Plank, M.J. Bishop, S.A. Niederer, Personalized computational modeling of left atrial geometry and transmural myofiber architecture, *Med. Image Anal.* 47 (2018) 180–190.
- [28] M. Hwang, S.S. Kwon, J. Wi, M. Park, H.S. Lee, J.S. Park, Y.S. Lee, E.B. Shim, H.N. Pak, Virtual ablation for atrial fibrillation in personalized in-silico three-dimensional left atrial modeling: comparison with clinical catheter ablation, *Prog. Biophys. Mol. Biol.* 116 (2014) 40–47.
- [29] O. Dossel, M.W. Krueger, F.M. Weber, M. Wilhelms, G. Seemann, Computational modeling of the human atrial anatomy and electrophysiology, *Med. Biol. Eng. Comput.* 50 (2012) 773–799.
- [30] S. Labarthe, J. Bayer, Y. Coudiere, J. Henry, H. Cochet, P. Jais, E. Vigmond, A bilayer model of human atria: mathematical background, construction, and assessment, *Europace* 16 (Suppl. 4) (2014) iv21–iv29.
- [31] C.H. Roney, J.D. Bayer, H. Cochet, M. Meo, R. Dubois, P. Jais, E.J. Vigmond, Variability in pulmonary vein electrophysiology and fibrosis determines arrhythmia susceptibility and dynamics, *PLoS Comput. Biol.* 14 (2018), e1006166.
- [32] C.H. Roney, J.D. Bayer, S. Zahid, M. Meo, P.M. Boyle, N.A. Trayanova, M. Haissaguerre, R. Dubois, H. Cochet, E.J. Vigmond, Modelling methodology of atrial fibrosis affects rotor dynamics and electrograms, *Europace* 18 (2016) iv146–iv155.
- [33] C.H. Roney, C.D. Cantwell, J.D. Bayer, N.A. Qureshi, P.B. Lim, J.H. Tweedy, P. Kanagaratnam, N.S. Peters, E.J. Vigmond, F.S. Ng, Spatial resolution requirements for accurate identification of drivers of atrial fibrillation, *Circ. Arrhythm. Electrophysiol.* 10 (2017), e004899.
- [34] M. Saha, C.H. Roney, J.D. Bayer, M. Meo, H. Cochet, R. Dubois, E.J. Vigmond, Wave-length and fibrosis affect phase singularity locations during atrial fibrillation, *Front. Physiol.* 9 (2018) 1207.
- [35] J.D. Bayer, C.H. Roney, A. Pashaei, P. Jais, E.J. Vigmond, Novel radiofrequency ablation strategies for terminating atrial fibrillation in the left atrium: a simulation study, *Front. Physiol.* 7 (2016) 108.
- [36] R.S. Oakes, T.J. Badger, E.G. Kholmovski, N. Akoum, N.S. Burgon, E.N. Fish, J.J. Blauer, S.N. Rao, E.V. DiBella, N.M. Segerson, M. Daccarett, J. Windfelder, C.J. McGann, D. Parker, R.S. MacLeod, N.F. Marrouche, Detection and quantification of left atrial structural remodeling with delayed-enhancement magnetic resonance imaging in patients with atrial fibrillation, *Circulation* 119 (2009) 1758–1767.
- [37] P.M. Boyle, S. Zahid, N.A. Trayanova, Towards personalized computational modelling of the fibrotic substrate for atrial arrhythmia, *Europace* 18 (2016) iv136–iv145.
- [38] S. Zahid, H. Cochet, P.M. Boyle, E.L. Schwarz, K.N. Whyte, E.J. Vigmond, R. Dubois, M. Hocini, M. Haissaguerre, P. Jais, N.A. Trayanova, Patient-derived models link reentrant driver localization in atrial fibrillation to fibrosis spatial pattern, *Cardiovasc. Res.* 110 (2016) 443–454.

- [39] E. Vigmond, A. Pashaei, S. Amraoui, H. Cochet, M. Hassaguerre, Percolation as a mechanism to explain atrial fractionated electrograms and reentry in a fibrosis model based on imaging data, *Heart Rhythm*. 13 (2016) 1536–1543.
- [40] M.W. Krueger, V. Schmidt, C. Tobón, F.M. Weber, C. Lorenz, D.U.J. Keller, H. Barschdorf, M. Burdumy, P. Neher, G. Plank, K. Rhode, G. Seemann, D. Sanchez-Quintana, J. Saiz, R. Razavi, O. Dössel, Modeling atrial fiber orientation in patient-specific geometries: a semi-automatic rule-based approach, *Functional Imaging and Modeling of the Heart*, Springer, Berlin Heidelberg 2011, pp. 223–232.
- [41] J. Zhao, B.J. Hansen, T.A. Csepe, P. Lim, Y. Wang, M. Williams, P.J. Mohler, P.M. Janssen, R. Weiss, J.D. Hummel, V.V. Fedorov, Integration of high-resolution optical mapping and 3-dimensional micro-computed tomographic imaging to resolve the structural basis of atrial conduction in the human heart, *Circ. Arrhythm. Electrophysiol.* 8 (2015) 1514–1517.
- [42] F. Pashakhanloo, D.A. Herzka, H. Ashikaga, S. Mori, N. Gai, D.A. Bluemke, N.A. Trayanova, E.R. McVeigh, Myofiber architecture of the human atria as revealed by submillimeter diffusion tensor imaging, *Circ. Arrhythm. Electrophysiol.* 9 (2016), e004133.
- [43] H. Lombaert, J.M. Peyrat, P. Croisille, S. Rapacchi, L. Fanton, F. Chieret, P. Clarysse, I. Magnin, H. Delingette, N. Ayache, Human atlas of the cardiac fiber architecture: study on a healthy population, *IEEE Trans. Med. Imaging* 31 (2012) 1436–1447.
- [44] M. Paul, D.W. Burt, J.E. Krieger, N. Nakamura, V.J. Dzau, Tissue specificity of renin promoter activity and regulation in mice, *Am. J. Phys.* 262 (1992) E644–E650.
- [45] T.H. Lye, K.P. Vincent, A.D. McCulloch, C.P. Hendon, Tissue-specific optical mapping models of swine atria informed by optical coherence tomography, *Biophys. J.* 114 (2018) 1477–1489.
- [46] M. Haissaguerre, P. Jais, D.C. Shah, A. Takahashi, M. Hocini, G. Quiniou, S. Garrigue, A. Le Mouroux, P. Le Metayer, J. Clementy, Spontaneous initiation of atrial fibrillation by ectopic beats originating in the pulmonary veins, *N. Engl. J. Med.* 339 (1998) 659–666.
- [47] H. Cochet, R. Dubois, S. Yamashita, N. Al Jefairi, B. Berte, J.M. Sellal, D. Hooks, A. Frontera, S. Amraoui, A. Zemoura, A. Denis, N. Derval, F. Sacher, O. Corneloup, V. Latrabe, S. Clement-Guinaudeau, J. Relan, S. Zahid, P.M. Boyle, N.A. Trayanova, O. Bernus, M. Montaudon, F. Laurent, M. Hocini, M. Haissaguerre, P. Jais, Relationship between fibrosis detected on late gadolinium-enhanced cardiac magnetic resonance and re-entrant activity assessed with electrocardiographic imaging in human persistent atrial fibrillation, *JACC Clin Electrophysiol* 4 (2018) 17–29.
- [48] D. Linz, A.D. Elliott, M. Hohl, V. Malik, U. Schotten, D. Dobrev, S. Nattel, M. Bohm, J. Floras, D.H. Lau, P. Sanders, Role of autonomic nervous system in atrial fibrillation, *Int. J. Cardiol.* (2018) <https://doi.org/10.1016/j.ijcard.2018.11.091> Epub ahead of print.
- [49] Y. Gao, Y. Gong, L. Xia, Simulation of atrial fibrosis using coupled myocyte-fibroblast cellular and human atrial models, *Comput Math Methods Med.* 2017 (2017) 9463010.
- [50] R. Morgan, M.A. Colman, H. Chubb, G. Seemann, O.V. Aslanidi, Slow conduction in the border zones of patchy fibrosis stabilizes the drivers for atrial fibrillation: insights from multi-scale human atrial modeling, *Front. Physiol.* 7 (2016) 474.
- [51] H. Fuller, F. Justo, B.D. Nearing, K.M. Kahlig, S. Rajamani, L. Belardinelli, R.L. Verrier, Eleclazine, a new selective cardiac late sodium current inhibitor, confers concurrent protection against autonomically induced atrial premature beats, repolarization alternans and heterogeneity, and atrial fibrillation in an intact porcine model, *Heart Rhythm*. 13 (2016) 1679–1686.
- [52] R.L. Verrier, H. Fuller, F. Justo, B.D. Nearing, S. Rajamani, L. Belardinelli, Unmasking atrial repolarization to assess alternans, spatiotemporal heterogeneity, and susceptibility to atrial fibrillation, *Heart Rhythm*. 13 (2016) 953–961.
- [53] S.M. Narayan, M.R. Franz, P. Clopton, E.J. Pruvot, D.E. Krummen, Repolarization alternans reveals vulnerability to human atrial fibrillation, *Circulation* 123 (2011) 2922–2930.
- [54] K.C. Chang, J.D. Bayer, N.A. Trayanova, Disrupted calcium release as a mechanism for atrial alternans associated with human atrial fibrillation, *PLoS Comput. Biol.* 10 (2014), e1004011.
- [55] K.C. Chang, N.A. Trayanova, Mechanisms of arrhythmogenesis related to calcium-driven alternans in a model of human atrial fibrillation, *Sci. Rep.* 6 (2016) 36395.
- [56] S.M. Narayan, D.E. Krummen, W.J. Rappel, Clinical mapping approach to diagnose electrical rotors and focal impulse sources for human atrial fibrillation, *J. Cardiovasc. Electrophysiol.* 23 (2012) 447–454.
- [57] S.M. Narayan, D.E. Krummen, K. Shivkumar, P. Clopton, W.J. Rappel, J.M. Miller, Treatment of atrial fibrillation by the ablation of localized sources: CONFIRM (Conventional Ablation for Atrial Fibrillation With or Without Focal Impulse and Rotor Modulation) trial, *J. Am. Coll. Cardiol.* 60 (2012) 628–636.
- [58] M. Haissaguerre, M. Hocini, A. Denis, A.J. Shah, Y. Komatsu, S. Yamashita, M. Daly, S. Amraoui, S. Zellerhoff, M.Q. Picat, A. Quotb, L. Jesel, H. Lim, S. Ploux, P. Bordachar, G. Attuel, V. Meillet, P. Ritter, N. Derval, F. Sacher, O. Bernus, H. Cochet, P. Jais, R. Dubois, Driver domains in persistent atrial fibrillation, *Circulation* 130 (2014) 530–538.
- [59] J.B. Hakim, M.J. Murphy, N.A. Trayanova, P.M. Boyle, Arrhythmia dynamics in computational models of the atria following virtual ablation of re-entrant drivers, *Europace* 20 (2018) iii45–iii54.
- [60] E.P. Gerstenfeld, D.J. Callans, S. Dixit, A.M. Russo, H. Nayak, D. Lin, W. Pulliam, S. Siddique, F.E. Marchlinski, Mechanisms of organized left atrial tachycardias occurring after pulmonary vein isolation, *Circulation* 110 (2004) 1351–1357.
- [61] E.G. Daoud, R. Weiss, R. Augostini, J.D. Hummel, S.J. Kalbfleisch, J.M. Van Deren, G. Dawson, K. Bowman, Proarrhythmia of circumferential left atrial lesions for management of atrial fibrillation, *J. Cardiovasc. Electrophysiol.* 17 (2006) 157–165.
- [62] N. Ad, S.D. Holmes, A.J. Rongione, V. Badhwar, L. Wei, L.M. Fornaresio, P.S. Massimiano, The long-term safety and efficacy of concomitant Cox maze procedures for atrial fibrillation in patients without mitral valve disease, *J. Thorac. Cardiovasc. Surg.* (2018) <https://doi.org/10.1016/j.jtcvs.2018.09.131> Epub ahead of print.
- [63] J.L. Cox, A. Churyla, S.C. Malaisrie, D.T. Pham, J. Kruse, O.N. Kisliitsina, McCarthy PM, A hybrid maze procedure for long-standing persistent atrial fibrillation, *Ann. Thorac. Surg.* 107 (2) (Feb. 2019) 610–618.
- [64] R.T. Carrick, B.E. Benson, J.H. Bates, P.S. Spector, Prospective, tissue-specific optimization of ablation for multiwavelet reentry: predicting the required amount, location, and configuration of lesions, *Circ. Arrhythm. Electrophysiol.* 9 (2016).
- [65] C.T. January, L.S. Wann, J.S. Alpert, H. Calkins, J.E. Cigarroa, J.C. Cleveland Jr., J.B. Conti, P.T. Ellinor, M.D. Ezekowitz, M.E. Field, K.T. Murray, R.L. Sacco, W.G. Stevenson, P.J. Tchou, C.M. Tracy, C.W. Yancy, American College of Cardiology/American Heart Association Task Force on Practice G, 2014 AHA/ACC/HRS guideline for the management of patients with atrial fibrillation: a report of the American College of Cardiology/American Heart Association Task Force on Practice Guidelines and the Heart Rhythm Society, *J. Am. Coll. Cardiol.* 64 (2014) e1–76.
- [66] E.P. Scholz, P. Carrillo-Bustamante, F. Fischer, M. Wilhelms, E. Zitron, O. Dossel, H.A. Katus, G. Seemann, Rotor termination is critically dependent on kinetic properties of I_{kur} inhibitors in an in silico model of chronic atrial fibrillation, *PLoS One* 8 (2013), e83179.
- [67] H. Ni, D.G. Whittaker, W. Wang, W.R. Giles, S.M. Narayan, H. Zhang, Synergistic anti-arrhythmic effects in human atria with combined use of sodium blockers and acacetin, *Front. Physiol.* 8 (2017) 946.
- [68] M. Aguilar, J. Feng, E. Vigmond, P. Comtois, S. Nattel, Rate-dependent role of I_{Kur} in human atrial repolarization and atrial fibrillation maintenance, *Biophys. J.* 112 (2017) 1997–2010.
- [69] M. Varela, M.A. Colman, J.C. Hancox, O.V. Aslanidi, Atrial heterogeneity generates reentrant substrate during atrial fibrillation and anti-arrhythmic drug action: mechanistic insights from canine atrial models, *PLoS Comput. Biol.* 12 (2016), e1005245.
- [70] D.G. Whittaker, M.A. Colman, H. Ni, J.C. Hancox, H. Zhang, Human atrial arrhythmogenesis and sinus bradycardia in KCNQ1-linked short QT syndrome: insights from computational modelling, *Front. Physiol.* 9 (2018) 1402.
- [71] C.D. Cantwell, Y. Mohamied, K.N. Tzortzis, S. Garasto, C. Houston, R.A. Chowdhury, F.S. Ng, A.A. Bharath, N.S. Peters, Rethinking multiscale cardiac electrophysiology with machine learning and predictive modelling, *Comput. Biol. Med.* 104 (Jan. 2019) 339–351.
- [72] S. Andalám, H. Ramanna, A. Malik, P. Roop, N. Patel, M.L. Trew, Hybrid automata models of cardiac ventricular electrophysiology for real-time computational applications, *Conf Proc IEEE Eng Med Biol Soc.* 2016 (2016) 5595–5598.